JOURNAL OF GUIDANCE, CONTROL, AND DYNAMICS
Vol. 15, No. 3, May-June 1992

Experiment of a Noncollocated Controller for Wave Cancellation

Hironori Fujii* and Toshiyuki Ohtsuka†
Tokyo Metropolitan Institute of Technology, Hino, Tokyo 191, Japan

Wave-absorbing control for vibration suppression of flexible space structures is demonstrated experimentally. The experimental model is a hung flexible beam with a sensor and a noncollocated torque actuator. The wave-absorbing control employs partial differential equations as the mathematical model of structural dynamics, and the controller can be designed without any use of the modal expansion. Thus, the control is free from the crucial truncation effect. The structural vibration is expressed in terms of propagating disturbances in the frequency domain. The control forces are applied to eliminate outgoing waves at the boundaries of the structure. The controller is implemented in the form of a nonrecursive digital filter. Details of the controller implementation are discussed, including the digital filter as a compensator, filter truncation, and the hardware. Experimental results show satisfactory performance of the controller and good agreement with the performance predicted analytically.

I. Introduction

LARGE space structures (LSS) will be inevitably flexible in their structure, and their structural vibration will be easily excited. Therefore, control techniques of structural vibration are necessary to satisfy performance of LSS. Most of the studies on the control problem of LSS employ the dynamic model with a discretized description for flexible structures that are inherently distributed parameter systems. The discretization is usually employed to adopt the conventional state-space method. Methods free from the discretization are natural and suitable to the control of such distributed parameter systems as the LSS.

This paper treats through the experiment the wave-absorbing control for vibration suppression of flexible structures. The wave-absorbing control employs partial differential equations as the mathematical model of structural dynamics to design the controller, and the discretization method is not employed in the analyses. The controller obtained is thus free from the crucial truncation effect. The equations are Laplace transformed with respect to time to describe the structural responses in terms of propagating disturbances in the frequency domain. Boundary conditions of the system are expressed as relations between incoming waves, outgoing waves, and external control forces at the boundaries. External control forces are applied to eliminate outgoing waves at the boundaries. Resulting closed-loop behavior of the system shows drastic improvement for disturbance attenuation in comparison with open-loop behavior.

The concept of the traveling wave approach is applied to the control problem of LSS by von Flotow.[1-3] He introduces the viewpoint that the elastic response of LSS may be aptly viewed in terms of the disturbance propagation characteristics of the structure. Active vibration isolation by cancelling traveling waves based on the same concept is studied in Refs. 4-8. The technique aims to isolate one part of a structure from disturbances excited elsewhere in the structure. Actuators are located at midpoints of structural members and cancel passing disturbances so that the disturbances do not disturb downstream portions. A generic description of the traveling wave control for structural networks is given in Ref. 9. Miller et al. apply the traveling wave approach to power flow in structural networks[10] and introduce H_2-optimal control of power flow at structural junctions.[11,12] H_∞-optimal control of power flow is discussed by MacMartin and Hall,[13,14] where the traveling wave approach is employed in order to obtain the driving point mobility of a structure. Reference 15 discusses minimization of wave reflection in the H_∞ sense. From these analyses, it is shown that a transfer function model of a distributed parameter system results in a controller of an irrational transfer function, which can be realized only approximately over a finite bandwidth.

Some studies are devoted to examine experimentally ideal controllers realized approximately through the use of analog circuits[2,8,12,14] or a recursive digital filter.[5] This paper tries to implement the ideal controller in the form of a nonrecursive digital filter and verifies validity of the control in the experiment. Results of the experiment exhibit satisfactory performance of the controller, and good agreement is attained concerning its performance in comparison with that predicted analytically.

II. Hardware Setup

A 1.20-m-long aluminum beam 15.0 mm in width and 1.0 mm in thickness is employed as a flexible structure in this experiment. The bending rigidity and the mass per unit length of the beam are 9.11×10^{-2} N·m^2 and 4.04×10^{-2} kg/m, respectively. As illustrated in Fig. 1, the beam is vertically sus-

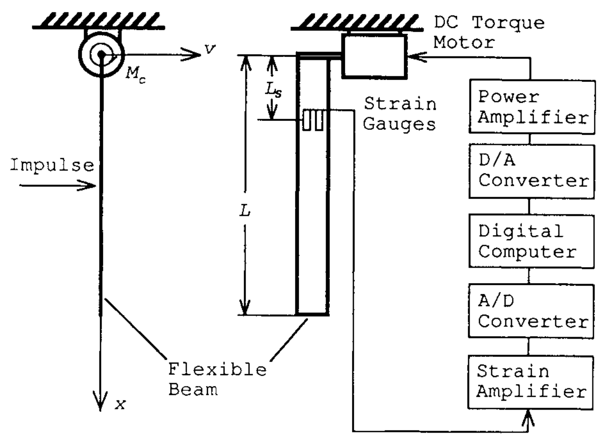

Fig. 1 Model configuration.

Received April 8, 1991; revision received Aug. 25, 1991; accepted for publication Sept. 25, 1991.

*Professor, Department of Aerospace Engineering. Member AIAA.

†Graduate Student, Department of Aerospace Engineering. Student Member AIAA.

pended from a support structure in such a way as to allow free vibration in the vertical plane, with the upper end fixed to the shaft of a dc torque motor and the lower end free. The DC torque motor is the actuator to control reflection of traveling waves at its position.

Four strain gauges are located to form a full bridge at distance $L_s = 0.199$ m from the upper end. The gauges are equipped to sense bending moment of the beam. The output of the full bridge is amplified by a strain amplifier and is put into a digital computer, NEC PC-9801RA, through an analog-to-digital (A/D) converter at a sampling rate of 1 kHz. The digital computer processes the sensor data under the control law and determines the control input as a voltage to put out through a digital-to-analog (D/A) converter. A power amplifier converts the output voltage of the D/A converter into a current proportional to the voltage and drives the DC torque motor.

The disturbance source to the flexible structure is given by a hammer. The hammer applies impulsive force to the beam at a position ($L_f = 0.466$ m) lower than the sensor position. The disturbance generated by the excitation arrives at the actuator position after passing the sensor position.

Sensor signal, control signal, and excitation signal are stored in the computer. Analysis of experimental results is carried out in the frequency domain utilizing the fast Fourier transform (FFT) of each data. Controller performance is evaluated in terms of the transfer function from the excitation force to the sensor output.

III. Controller Design

System Model

The predominant flexibility of the beam leads to horizontal deflections $v(x,t)$ in a vertical plane. This behavior is well described by the partial differential equation (damping and tensile force are ignored)

$$EI\frac{\partial^4(x,t)}{\partial x^4} + \rho\frac{\partial^2 v(x,t)}{\partial t^2} = F(x,t) \tag{1}$$

together with the boundary conditions

$$v(0,t) = 0, \qquad EI\frac{\partial^2 v}{\partial x^2}(0,t) = M_c(t) \tag{2a}$$

$$EI\frac{\partial^2 v}{\partial x^2}(L,t) = 0, \qquad EI\frac{\partial^3 v}{\partial x^3}(L,t) = 0 \tag{2b}$$

where EI is the bending rigidity and ρ the mass per unit length of the beam. The control torque M_c applied to the root of the beam is included in the boundary conditions and not in the external force $F(x,t)$.

After Laplace transformation, Eq. (1) is transformed into an ordinary differential equation (in order to avoid new symbols, the transformed variables hereafter have the same notation as their time-dependent equivalents):

$$\frac{\mathrm{d}^4 v}{\mathrm{d}x^4}(x,s) + \frac{\rho s^2}{EI}v(x,s) = 0 \tag{3}$$

It is convenient to set $F(x,s) = 0$ in Eq. (3) in order to describe the separate processes of wave propagation and wave generation by external force. The general solution of Eq. (3) is described as

$$v(x,s) = C_1(s)e^{j\lambda(s)x} + C_2(s)e^{\lambda(s)x} + C_3(s)e^{-j\lambda(s)x} + C_4(s)e^{-\lambda(s)x} \tag{4}$$

where

$$\lambda(s) = \frac{1-j}{\sqrt{2}}\left(\frac{\rho}{EI}\right)^{1/4}\sqrt{s} \tag{5}$$

and the displacement of the beam, $v(x,s)$, consists of the following four wave modes:

$$a_1(x,s) = C_1(s)e^{j\lambda(s)x} \tag{6a}$$

$$a_2(x,s) = C_2(s)e^{\lambda(s)x} \tag{6b}$$

$$b_1(x,s) = C_3(s)e^{-j\lambda(s)x} \tag{6c}$$

$$b_2(x,s) = C_4(s)e^{-\lambda(s)x} \tag{6d}$$

where a_1 and a_2 represent waves traveling in the negative direction of the beam and denote incoming waves at the upper end of the beam ($x = 0$). The wave modes b_1 and b_2 travel in the positive direction and denote outgoing waves at the upper end. It should be noted that values of $\lambda(s)$ and wave modes are not real numbers when s is a positive real number; this implies that the time domain expression of each wave mode is a complex-valued function of time. Another expression of wave modes is possible to avoid inconvenience in dealing with the transfer functions of complex valued impulse responses.[15,16] However, other expressions than Eq. (6) result in a nondiagonal transfer function matrix of wave modes and, consequently, disables the separate expression of propagation of wave modes. Therefore, we employ Eq. (6) as the expression of wave modes for the present analysis.

The relationship between wave modes at two points on the beam is obtained from Eqs. (6) as follows:

$$w(l_1,s) = \begin{bmatrix} e^{j\lambda(l_1-l_0)} & & & \\ & e^{\lambda(l_1-l_0)} & & \\ & & e^{-j\lambda(l_1-l_0)} & \\ & & & e^{-\lambda(l_1-l_0)} \end{bmatrix} w(l_0,s) \tag{7}$$

where the vector w is defined as

$$w = [a_1,\ a_2,\ b_1,\ b_2]^T \tag{8}$$

It is seen from Eq. (7) that each wave mode travels independently of others, and transfer functions from the upstream to the downstream of the wave modes are causal.

Differentiation of Eq. (4) with respect to x leads one to express the state of the beam in terms of the wave modes as follows:

$$y(x,s) = \begin{bmatrix} 1 & 1 & 1 & 1 \\ j\lambda & \lambda & -j\lambda & -\lambda \\ -M_0 & M_0 & -M_0 & M_0 \\ -j\lambda M_0 & \lambda M_0 & j\lambda M_0 & -\lambda M_0 \end{bmatrix} w(x,s) \tag{9}$$

where $M_0 = \lambda^2(s)EI$, and the cross-sectional state vector $y(x,s)$ is defined as

$$y = [v,\theta,M,V]^T \tag{10}$$

Notations employed are $\theta = \mathrm{d}v/\mathrm{d}x$ is the slope, $M = EI(\mathrm{d}^2v/\mathrm{d}x^2)$ the internal bending moment, and $V = EI(\mathrm{d}^3v/\mathrm{d}x^3)$ the internal shear force.

To analyze the beam dynamics at the upper end of the beam in wave mode coordinates, the boundary conditions in terms of the cross-sectional state vector y at $x = 0$ are introduced in matrix form

$$\begin{bmatrix} v(0,s) \\ M(0,s) \end{bmatrix} = \begin{bmatrix} 1 & 0 & 0 & 0 \\ 0 & 0 & 1 & 0 \end{bmatrix} y(0,s) = \begin{bmatrix} 0 \\ M_c(s) \end{bmatrix} \tag{11}$$

and transformed into wave mode coordinates through the use of Eq. (9)

$$\begin{bmatrix} 1 & 1 & 1 & 1 \\ -M_0 & M_0 & -M_0 & M_0 \end{bmatrix} w(0,s) = \begin{bmatrix} 0 \\ M_c(s) \end{bmatrix} \tag{12}$$

Partitioning $w(0,s)$ into the incoming $a(0,s)$ and the outgoing $b(0,s)$ wave modes, we obtain from Eq. (12) the following relation:

$$\begin{bmatrix} b_1 \\ b_2 \end{bmatrix} = \begin{bmatrix} -1 & 0 \\ 0 & -1 \end{bmatrix} \begin{bmatrix} a_1 \\ a_2 \end{bmatrix} + \begin{bmatrix} -1 \\ 1 \end{bmatrix} \frac{M_c(s)}{2M_0} \tag{13}$$

or, in general,

$$b(0,s) = Sa(0,s) + BM_c(s) \tag{14}$$

It is seen from Eq. (13) that the outgoing wave modes $b(0,s)$ are produced by the reflection of the incoming wave modes $a(0,s)$ and by control torque $M_c(s)$. The reflection coefficient S of the incoming wave modes shows that the phase of the outgoing waves shifts π radians from that of the incoming waves.

Wave-Absorbing Controller Design

The wave-absorbing controller is designed through use of Eq. (13), but is limited to the following form in this experiment:

$$M_c(s) = C(s)M(L_s,s) \tag{15}$$

where the control torque $M_c(s)$ is applied in response to the bending moment $M(L_s,s)$ at the sensor position. The sensor output is expressed in terms of the wave modes at the actuator position using Eqs. (7–9), and the closed-loop scattering behavior at the actuator position is obtained as follows from Eqs. (13) and (15):

$$b(0,s) = S_{cl}a(0,s) \tag{16}$$

where $S_{cl}(s)$ is the closed-loop scattering matrix

$$\begin{aligned} S_{cl} &= \{I - C(s)M_0(s)B[-e^{-j\lambda L_s} \; e^{-\lambda L_s}]\}^{-1} \\ &\quad \times \{-I + C(s)M_0(s)B[-e^{j\lambda L_s} \; e^{\lambda L_s}]\} \\ &= \frac{1}{2 - C(s)(e^{-\lambda L_s} + e^{-j\lambda L_s})} \\ &\quad \times \begin{bmatrix} -2 + C(s)(e^{j\lambda L_s} + e^{-\lambda L_s}) & -C(s)(e^{\lambda L_s} - e^{-\lambda L_s}) \\ -C(s)(e^{j\lambda L_s} - e^{-j\lambda L_s}) & -2 + C(s)(e^{\lambda L_s} + e^{-j\lambda L_s}) \end{bmatrix} \end{aligned} \tag{17}$$

In the case of the controller $C(s)$ which leads to $S_{cl} = 0$ exists, it is clear from Eq. (16) that any incoming waves $a(0,s)$ are canceled, and the outgoing wave modes $b(0,s)$ are zero identically at the boundary. All elements of S_{cl}, however, cannot be set zero at the same time over all frequency ranges in this case, and $C(s)$ which leads to $S_{cl(1,1)} = 0$ is selected in order to reduce the dominant elements a_1 and b_1 in vibration of the model as follows:

$$\begin{aligned} C(s) &= \frac{2}{e^{j\lambda L_s} + e^{-\lambda L_s}} \\ &= \frac{\cos\sqrt{\alpha s} - j\sin\sqrt{\alpha s}}{\cosh\sqrt{\alpha s}} \end{aligned} \tag{18}$$

where

$$\alpha = \frac{L_s^2}{2}\sqrt{\frac{\rho}{EI}} \tag{19}$$

The controller transfer function $C(s)$ is analytic in the open right half of the complex plane, namely, it is causal. However, $C(s)$ is not a real number on the positive real axis as well as $\lambda(s)$ and wave modes, i.e., the impulse response of $C(s)$ is a complex-valued function as shown in Fig. 2. A transfer function with a complex-valued impulse response cannot be realized by any means. Moreover, $C(s)$ consists of irrational terms, which can be realized only approximately over a finite bandwidth. Some approximation techniques are required in order to implement the controller transfer function, as presented in the next section. It should be noted, therefore, that the present controller design does not depend on a modal model of the system and is free from the truncation effect of modes, whereas approximate implementation of the controller may degrade control performance.

IV. Experimental Results

Implementation of the Control Law

Although the ideal controller in Eq. (18) is causal in contrast to controllers discussed in Refs. 11–14, it can neither be implemented exactly as the noncausal controllers because of its complex-valued impulse response. Controller transfer function must have a real-valued impulse response in order to be implemented. We have to find an approximate transfer function of $C(s)$ with a real-valued impulse response. One possible approximation $C_{a1}(s)$ is the part of $C(s)$ with a real-valued impulse response as follows:

$$C_{a1}(s) = \frac{\cos\sqrt{\alpha s}}{\cosh\sqrt{\alpha s}} \tag{20}$$

The basis of this approximation is that the neglected term $\sin\sqrt{\alpha s}$ has small magnitude in a low-frequency range, and $C_{a1}(s)$ gives the minimum error approximation of $C(s)$ in the L_2 sense. However, the gain of $C_{a1}(s)$ is identically equal to 1 on the imaginary axis, whereas the gain of $C(j\omega)$ approaches 2 asymptotically from below as the angular frequency ω increases. Satisfactory performance is not to be obtained with $C_{a1}(s)$ because of its lower gain than the ideal controller. The following modified transfer function is able to regain enough gain in a low-frequency range:

$$C_{a2}(s) = 2e^{-\sqrt{\alpha s}}\cos\sqrt{\alpha s} \tag{21}$$

The transfer function in Eq. (21) results from Eq. (20) ignoring the exponential term $e^{-\sqrt{\alpha s}}$ in the hyperbolic function, which represents the contribution of the evanescent wave and reduces the gain at low frequency. The gain of $C_{a2}(j\omega)$ is 2 at $\omega = 0$ and approaches 1 asymptotically from above as ω increases. Although the global behavior of $|C_{a2}(j\omega)|$ is different from $|C(j\omega)|$, $C_{a2}(s)$ gives a reasonable approximation of $C(j\omega)$ in a finite frequency range. The sensor output is filtered by a

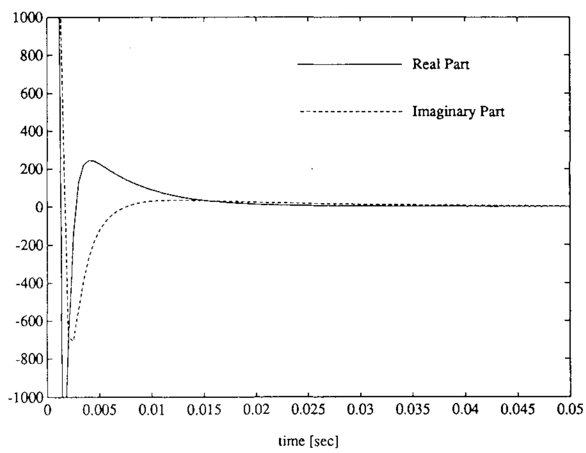

Fig. 2 Impulse response of the ideal controller.

first-order high-pass filter in order to avoid instability due to the slight offset of the strain gauges, and the resultant transfer function $C_a(s)$ to be implemented is given as follows:

$$C_a(s) = \frac{2sTe^{-\sqrt{\alpha s}}\cos\sqrt{\alpha s}}{1+sT} \tag{22}$$

where the time constant T is selected as 1000 s to set the cutoff frequency at 1.6×10^{-4} Hz. This procedure for approximation is ad hoc rather than systematic. It may be noted that a more systematic approach is to design controllers through a certain optimization under constraints on causality[11-14] or to express wave modes in terms of only transfer functions with real-valued impulse responses.[15,16]

The controller transfer function $C_a(s)$ is implemented in the form of a digital filter in this experiment. If the transfer function is rational, the bilinear transform results in a recursive digital filter. However, the transfer function $C_a(s)$ is irrational, and its rational approximation is necessary to be transformed in order to design a recursive digital filter. We adopt not a recursive digital filter but a nonrecursive digital filter for its simple implementation. Calculation of the control input thus requires only sensor output during a finite time interval in the past. Order of the filter is selected as 16, and the sample interval T is set as 1 ms. The control input M_c is calculated by the digital filter in the form of a convolution in the time domain:

$$M_c(nT) = \sum_{i=0}^{N-1} h[i]M(L_s, nT-iT), \quad (n=0,1,2,3,\cdots) \tag{23}$$

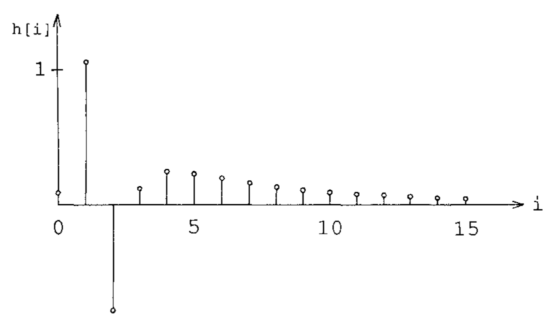

Fig. 3 Impulse response sequence of the digital filter.

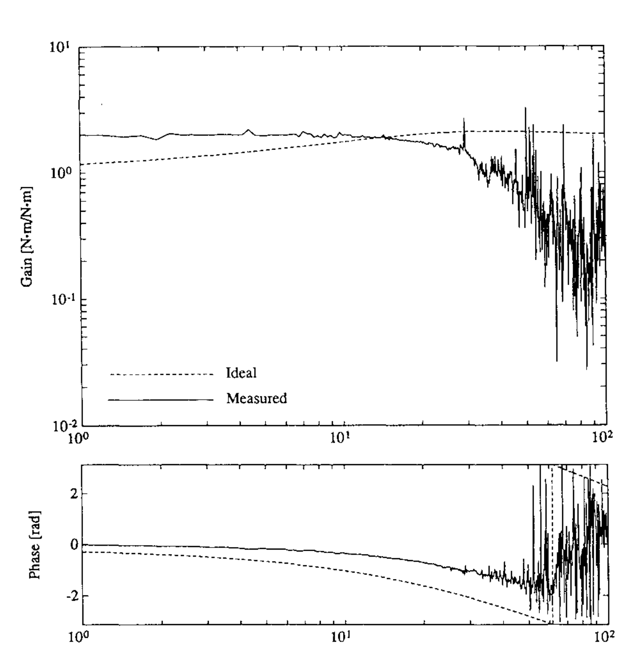

Fig. 4 Transfer functions of the ideal and implemented controllers.

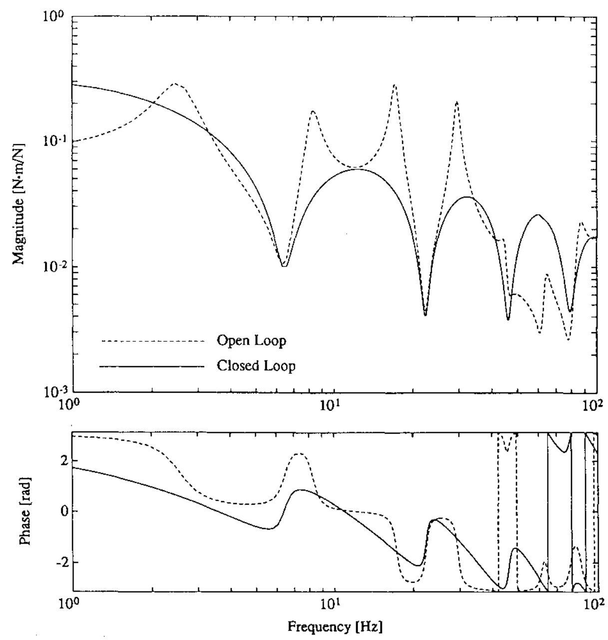

Fig. 5 Predicted transfer functions of the open loop and closed loop.

where $h[i]$ is the impulse response sequence of the digital filter and is determined through the use of an inverse discrete Fourier transform of the transfer function $C_a(j\omega)$:

$$h[i] = \frac{1}{N}\sum_{k=0}^{N-1} C_a\left(j\frac{2\pi k}{N}\right)e^{j2\pi ik/N}, \quad (i=0,1,2,\cdots,N-1) \tag{24}$$

It is assumed that the aliasing effect is negligible. The impulse response sequence $h[i]$ of the digital filter is shown in Fig. 3.

The transfer function of the ideal controller, Eqs. (18), and the measured transfer function of the implemented controller as in Eq. (23) are shown in Fig. 4. Although the global behavior of the gain of the measured transfer function is different from that of the ideal transfer function as expected from the approximation, both transfer functions are seen to have enough agreement in the frequency range below about 30 Hz. The gain of the implemented controller is small enough in the frequency range above 30 Hz where phase error is large. The discrepancy in phase and error in the high-frequency range is due to the filter truncation by the low order, which is imposed by the limitation of computational speed of the computer. The phase of the ideal controller lags proportionally to $\sqrt{\omega}$, which is due to the time lag required for wave propagation from the sensor position to the actuator position.

Predicted and Measured Transfer Functions

Figure 5 shows predicted open- and closed-loop transfer functions from the excitation force to the sensor output. The closed-loop transfer function is a response controlled by the ideal controller. The transfer functions are calculated by an exact solution of the Laplace-transformed equation of motion. Viscous damping ($c_1\partial v/\partial t$) and Kelvin-Voigt damping ($c_2\partial^5 v/\partial t\partial x^4$) are included in the calculation with damping coefficients $c_1=0.2$ (N·s/m^2) and $c_2=1\times10^{-5}$ (N·m^2·s), respectively. The result shows that the wave cancellation improves the structural response drastically.

Figure 6 shows measured open- and closed-loop transfer functions from the excitation force to the sensor output. Good agreement is seen in the magnitude between the computational and the experimental results in Figs. 5 and 6. Influence of the gravity dominates at about 1 Hz and is negligible at the frequency range higher than 2 Hz. Such unmodeled dynamics as the influence of the gravity and vibration of the support structure cause discrepancies in the phase between the computational and the experimental results. Nevertheless, the experi-

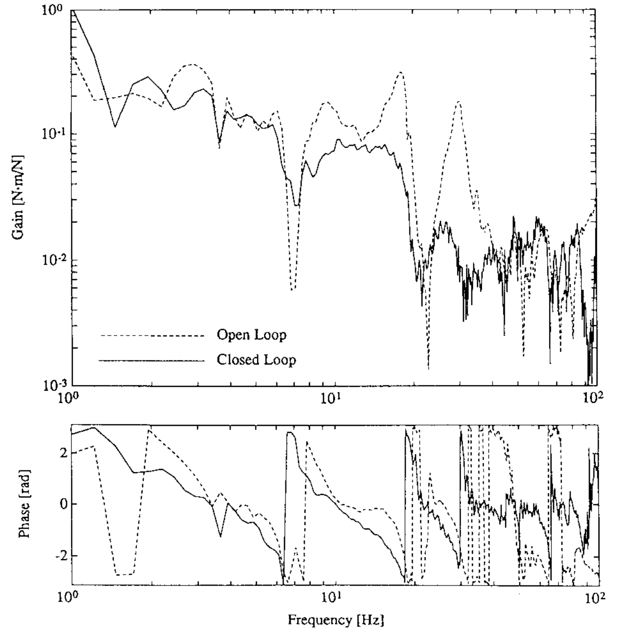

Fig. 6 Measured transfer functions of the open loop and closed loop.

mental result shows that the modes in 2–30 Hz are suppressed and assures that damping is augmented by the approximate implementation of the ideal controller.

V. Conclusions

This paper demonstrates experimentally a wave-absorbing control method for vibration suppression of flexible structures modeled as a hinged-free beam with a sensor and a noncollocated actuator. The control theory is applied to treat the vibration as superposed wave modes traveling in positive and negative directions and to suppress the vibration by cancelling outgoing vibratory wave modes at the actuator position. The controller is obtained from the theoretical analysis to set one dominant element of the scattering matrix zero at the controlled boundary of the model. The controller transfer function consists of irrational terms and has a complex-valued impulse response. The controller transfer function is approximated by a transfer function with a real-valued impulse response, and the approximate controller is implemented in the digital computer as a nonrecursive digital filter. Although the controller design does not depend on a modal model of the system and is free from the truncation effect of modes, approximate implementation of the controller may degrade control performance. Experimental results show that the wave-absorbing control suppresses vibration of the model satisfactorily in spite of its approximate implementation, and it is concluded that effectiveness is experimentally verified for the present design of the wave-absorbing control.

Acknowledgments

The authors are grateful to Douglas G. MacMartin of Massachusetts Institute of Technology for his kind advice through this research. The authors also thank Ken Miyachi, Sei-ichi Anazawa, and Khoichi Matsuda of Tokyo Metropolitan Institute of Technology for their cooperation in constructing hardware, in programming software, and for discussion.

References

[1]von Flotow, A. H., "Travelling Wave Control for Large Spacecraft Structures," *Journal of Guidance, Control, and Dynamics*, Vol. 9, No. 4, 1986, pp. 462–468.

[2]von Flotow, A. H., and Schäfer, B., "Wave-Absorbing Controllers for a Flexible Beam," *Journal of Guidance, Control, and Dynamics*, Vol. 9, No. 6, 1986, pp. 673–680.

[3]von Flotow, A. H., "The Acoustic Limit of Control of Structural Dynamics," *Large Space Structures: Dynamics and Control*, edited by S. N. Atluri and A. K. Amos, Springer-Verlag, Berlin, Germany, 1988, pp. 213–237.

[4]Mace, B. R., "Active Control of Flexural Vibrations," *Journal of Sound and Vibration*, Vol. 114, No. 2, 1987, pp. 253–270.

[5]McKinnell, R. J., "Active Vibration Isolation by Cancelling Bending Waves," *Proceedings of the Royal Society of London*, Vol. A421, 1989, pp. 357–393.

[6]Kuehnle, A. U., "Control of Longitudinal Waves in a Rod with Voigt Damping," *Proceedings of American Control Conference*, Pittsburgh, PA, June 1989, pp. 200–205.

[7]Hagedorn, P., Wallaschek, J., and Chen, P., "Active Vibration Damping in Beams," *Proceedings of American Control Conference*, Pittsburgh, PA, June 1989, pp. 206–211.

[8]Pines, D. J., and von Flotow, A. H., "Active Control of Bending Wave Propagation," *Journal of Sound and Vibration*, Vol. 142, No. 3, 1990, pp. 391–412.

[9]Fujii, H., Ohtsuka, T., and Murayama, T., "Wave-Absorbing Control for Flexible Structures with Non-Collocated Sensors and Actuators," *Journal of Guidance, Control, and Dynamics* (to be published).

[10]Miller, D. W., and von Flotow, A. H., "A Traveling Wave Approach to Power Flow in Stuctural Networks," *Journal of Sound and Vibration*, Vol. 128, No. 1, 1989, pp. 145–162.

[11]Miller, D. W., Hall, S. R., and von Flotow, A. H., "Optimal Control of Power Flow at Structural Junctions," *Journal of Sound and Vibration*, Vol. 140, No. 3, 1990, pp. 475–497.

[12]Miller, D. W., and Hall, S. R., "Experimental Results Using Active Control of Travelling Wave Power Flow," *Journal of Guidance, Control, and Dynamics*, Vol. 14, No. 2, 1991, pp. 350–359.

[13]MacMartin D. G., and Hall, S. R., "Control of Uncertain Structures Using an H_∞ Power Flow Approach," *Journal of Guidance, Control, and Dynamics*, Vol. 14, No. 3, 1991, pp. 521–530.

[14]MacMartin, D. G., and Hall, S. R., "Structural Control Experiments Using An H_∞ Power Flow Approach," *Proceedings of the AIAA Guidance, Navigation, and Control Conference*, Portland, OR, Aug. 1990, pp. 1634–1644.

[15]Fujii, H., Matsuda, K., and Ohtsuka, T., "H_∞ Optimized Broadband Compensator for Wave-Absorbing Control," American Astronomical Society, Paper 91-377, AAS/AIAA Astrodynamics Specialist Conference, Durango, CO, Aug. 1991.

[16]Vaughan, D. R., "Application of Distributed Parameter Concepts to Dynamic Analysis and Control of Bending Waves," *Journal of Basic Engineering*, June 1968, pp. 157–166.